CRYSTAL STRUCTURES OF BINARY AND TERNARY COMPLEXES OF THYMIDYLATE SYNTHASE (ThyA) FROM *Mycobacterium tuberculosis*: INSIGHTS INTO SELECTIVITY AND INHIBITION

A Thesis

by

WAYNE DANIEL HARSHBARGER

Submitted to the Office of Graduate Studies of
Texas A&M University
in partial fulfillment of the requirements for the degree of

MASTER OF SCIENCE

August 2011

Major Subject: Chemistry

Crystal Structures of Binary and Ternary Complexes of

Thymidylate Synthase (ThyA) from *Mycobacterium tuberculosis:*

Insights into Selectivity and Inhibition

CRYSTAL STRUCTURES OF BINARY AND TERNARY COMPLEXES OF THYMIDYLATE SYNTHASE (ThyA) FROM *Mycobacterium tuberculosis*: INSIGHTS INTO SELECTIVITY AND INHIBITION

A Thesis

by

WAYNE DANIEL HARSHBARGER

Submitted to the Office of Graduate Studies of
Texas A&M University
in partial fulfillment of the requirements for the degree of

MASTER OF SCIENCE

Approved by:

Chair of Committee,	James Sacchettini
Committee Members,	David Barondeau
	Frank Raushel
	Tatyana Igumenova
Head of Department,	David Russell

August 2011

Major Subject: Chemistry

ABSTRACT

Crystal Structures of Binary and Ternary Complexes of Thymidylate Synthase (ThyA) from *Mycobacterium tuberculosis*: Insights into Selectivity and Inhibition.

(August 2011)

Wayne Daniel Harshbarger, B.S., Virginia Commonwealth University

Chair of Advisory Committee: Dr. James Sacchettini

Thymidylate synthase (TS), encoded by the ThyA gene, is essential for the growth and survival of Mycobacterium *tuberculosis* and therefore is a potential drug target. Thymidylate synthase binds both a substrate, 2'-deoxyuridine-5'monophosphate (dUMP) as well as a cofactor, (6R,S)-5,10-methylenetetrahydrofolate (mTHF), providing the ability to inhibit a single target by two separate classes of molecules. 5'-fluoro-2'-deoxyuridine-5'-monophosphate (FdUMP) is a very tight binding mechanism based inhibitor, shown to have a K_i of 2nM for Mtb TS. Pemetrexed and Raltitrexed are both anti-folates, targeting the cofactor binding site of thymidylate synthase.

The x-ray crystal structures of *Mycobacterium tuberculosis* thymidylate synthase were solved in the binary complexes ThyA-dUMP and ThyA-FdUMP at 2.5 Å and 2.4 Å resolutions, respectively. The ternary complex, ThyA-dUMP-Pemetrexed was solved to a resolution of 1.7 Å. The enzyme is comprised of 8

α-helices as well as 23% of the protein formed by β-sheets, including the dimer interface which is a β-sandwich. Examination of the dUMP binding site allowed the identification of key conserved residues that play a role in ligand binding and catalysis. Comparison of the dUMP-Pemetrexed ternary complex with that of the human crystal structure shows two fewer interactions in the Mtb enzyme. One is due to the replacement of a Met with a Val which doesn't allow hydrophobic interactions with the ring system of Pemetrexed, and the other is the replacement of an Asn with a Trp, depriving the Mtb protein of a hydrogen bond at the N7 of the pyrrolo ring.

A spectrophotometric assay that monitored DHF formation was used to determine the inhibition of Pemetrexed and Raltitrexed on Mtb TS. Both were verified as noncompetitive inhibitors, and Pemetrexed was found to have an IC_{50} of 17μM and a K_i of 16.8μM, while Raltitrexed had an IC_{50} of 3.5μM and a K_i of 3.2μM.

DEDICATION

To my daughter, Kayli, for being my biggest motivation.

To my wife, Amanda Harshbarger, for all her love and patience.

To my parents, John and Cynthia Harshbarger, for all their sacrifice and love.

To my siblings, Santina Thelen, Elijah Harshbarger, and James Harshbarger, for always being there for each other.

ACKNOWLEDGEMENTS

I would like to express thanks to my advisor, Dr. James Sacchettini, for his acceptance of me into his research group and giving me the opportunity to be involved in such exciting research. I would like to thank my committee members, Dr. David Barondeau, Dr. Frank Raushel, and Dr. Tatyana Igumenova, for contributing to my graduate studies and challenging me to develop my full potential as a scientist.

I would also like to thank Manchi Reddy for taking the time to assist me with data collection and processing. I would also like to thank the rest of the Sacchettini research group for their friendship and collaboration.

TABLE OF CONTENTS

Page

LIST OF FIGURES

FIGURE Page

LIST OF TABLES

1. INTRODUCTION: *Mycobacterium tuberculosis*

1.1 Global Tuberculosis

1.1.1 Tuberculosis Statistics

As of 1993, *Mycobacterium tuberculosis*, the bacteria responsible for tuberculosis, is a global health emergency, affecting one-third of the world's population. Tuberculosis ranks 2nd only to HIV among infectious killers worldwide(1). *M. tuberculosis* typically infects the lungs, but can infect any part of the body, and when left untreated kills 50% of its victims. Of the 2 billion people infected with latent TB, over 9 million become sick with the active form of the bacteria, which can be spread to infect others(2). The mortality due to infection is greater than 2 million annually, as reported by the World Health Organization. There are an increasing number of *Mycobacterium tuberculosis* strains that are becoming resistant to antibiotics due to patients stopping their medication too soon, incorrect prescriptions, and poor quality of drugs. These strains are referred to as multidrug-resistant tuberculosis (MDR TB) and in some cases extensively drug resistant (XDR TB), and emphasize the need to pursue discovery of novel therapeutics to combat this disease(3, 4). Evidence of tubercular decay has been found in the skulls and spines of Egyptian mummies, indicating that TB has been infecting humans for at least 4,000 years.

This thesis follows the style of Cancer Research.

1.1.2 Risk Factors

Tuberculosis can affect *anyone*, but there are specific factors that can increase your body's ability to become susceptible to the bacteria. A weakened immune system is a primary risk, and can be due to HIV infection, diabetes, chemotherapy for cancer, malnutrition, or age (Mayo Clinic). Tuberculosis is found most abundantly in South Africa, with 940 cases reported per 100,000 people, however huge areas of the world, including the Indian Subcontinent, Far East, China and the former Soviet Union, have rates between 100 and 300 per 100,000 people (Figure 1)(5).

TB Burden, 2006

	Incidence	Mortality
South Africa	940	218
India	168	28
Russian Federation	107	17
China	99	15
U.S	4.6	0.2

Rates per 100,000 Population

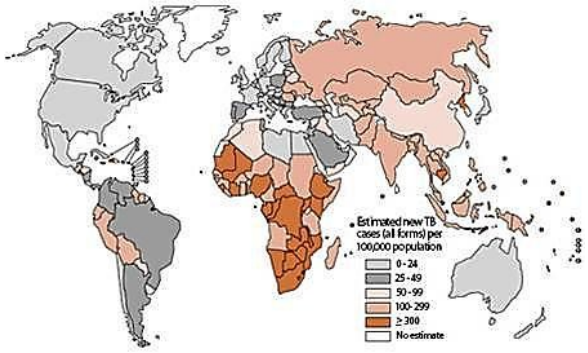

Figure 1- Global incidence and mortality of tuberculosis.

1.1.3 Symptoms, Diagnosis and Cost of Treatment

Infection by *Mycobacterium tuberculosis* can lead to symptoms such as being easily tired, high fever, sharp chest pain accompanied by a cough, spitting up blood, and night sweats. Tuberculosis most commonly infects the lungs, but

in 15% of patients it can be found to infect the lymph nodes, GI tract, or even bones and joints(6).

The Mantoux skin test can be used for identifying persons who are infected with TB. Approximately 0.1mL of purified protein derivative is injected under the skin which causes a delayed cellular hypersensitivity in persons infected. This is caused by re-stimulation of T-lymphocytes which have entered the bloodstream after being initially proliferated in response to infection. The result of a positive skin test is the appearance of a clearly defined, hard raised area at the point of injection (7-9).

Chest X-rays are often used as a diagnostic tool to rule out TB in patients who have tested positive to the skin test. Tuberculosis of the lungs is distinguishable by infiltrates or cavities, and often many small nodules throughout the lungs(6).

The only definitive way of determining infection is by a microbiological examination. A specimen from a patient believed to be infected is examined either by DNA amplification by polymerase chain reaction, smear exams, or a BACTEC culture for tuberculosis. A BACTEC culture uses enriched Middlebrook 7H12 ^{14}C labeled palmitic acid, in which mycobacterial growth can be detected by the utilization of ^{14}C and release of $^{14}CO_2$(10).

The world market for Tuberculosis drugs in 2006 was $370 million. In poor nations, a six month course of treatment can cost less than $20; however, in the US a two week treatment can cost as much as $200 (TBalliance.org).

1.1.4 Tuberculosis Drugs

There are four main first line TB drugs, which when taken in combination can kill Mtb in 6-18 months, depending on the prescription given. The first of these drugs, Isoniazid, is a pro-drug that is activated by the KatG enzyme of *Mycobacterium tuberculosis* to form an isonicotinoyl radical(11). This radical then reacts non-enzymatically with oxidized NAD^+ generating several 4-isonicotinoyl-NAD adducts, one of which then targets the NADH dependent enoyl-acyl carrier protein reductase, InhA, while a second adduct has been shown to inhibit DHFR (Figure 2)(12, 13). Binding to InhA inhibits the action of fatty acid synthase, ultimately stopping the production of mycolic acid which is used to make the bacterial cell wall. Resistance to Isoniazid has been shown to be caused by a mutation of Ser94, which disrupts the H-bonding network stabilizing NADH to InhA (14).

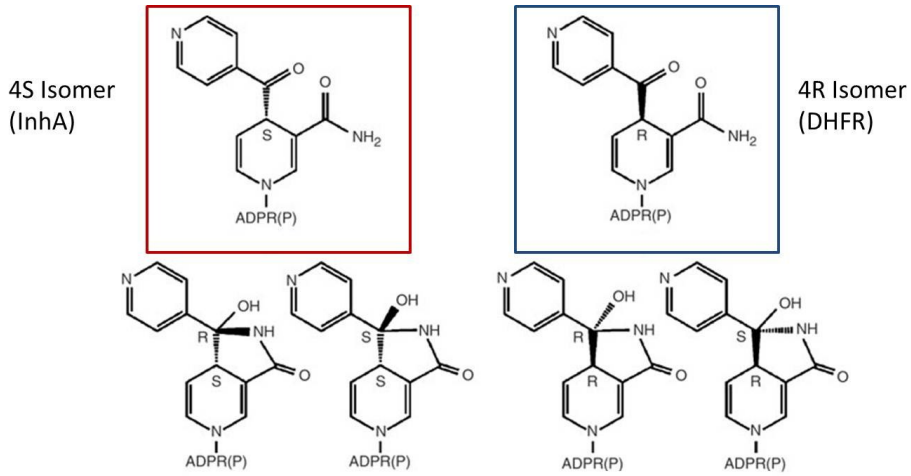

Figure 2- Isonicotinoyl-NAD adducts. Formed by Isoniazid after activation by KatG and non-enymatic oxidation by NAD^+. The 4S isomer has been shown to inhibit InhA, while the 4R isomer targets DHFR.

Pyrazinamide,also a pro-drug, is activated to its lethal form, pyrazinoic acid, by the enzyme pyrazinamidase. The mode of action is largely unclear, but it has been shown *in vitro* to inhibit the activity of (FAS)1, which is required for the synthesis of fatty acids(15). Resistance to pyrazinamide develops through mutations in pncA, the gene encoding pyrazinamidase(16). Pyrazinamide taken in combination with Isoniazide shortens the treatment time from 12-18 months, down to only six months. It does so by apparently killing a population of dormant bacteria that are not affected by the other first line drugs.

Ethambutol is a simple diamine molecule which limits bacterial growth without killing the bacteria. It works in synergy with other first line TB drugs and targets arabinosyl transferases, EmbA and MbbB, which are responsible for arabinogalactan biosynthesis, another component of the bacterial cell wall(17). The mycobacterial cell wall core consists of two layers; the outer layer is made of mycolic acids, while the inner layer consists of peptidoglycan. These two layers are held together by arabinogalactan (Figure3).

Rifampin is the most recently discovered first line antitubercular drug. It was discovered in 1966 and is a derivative of rifamycin B, an antibiotic produced by *Streptomyces mediterranei* (Figure 3)(18). Rifampin inhibits DNA-dependent RNA polymerase, leading to suppression of RNA synthesis(19). Mutations in the rpoB gene have been linked to rifampin resistance (20).

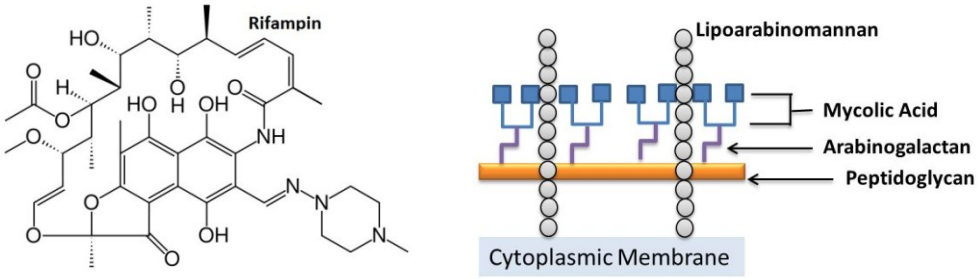

Figure 3- (Left) Rifampin, a first line TB antibiotic. (Right) A schematic of the bacterial cell wall. Mycolic acid synthesis is inhibited by Isoniazid, and arabinogalactan synthesis is inhibited by Ethambutol.

1.2 Thymidylate Synthase as a Drug Target

1.2.1 *De Novo* Pathway and Essentiality of ThyA

Thymidylate synthase, ThyA, is an essential enzyme in most organisms, catalyzing the final step in the *de novo* pathway for synthesis of thymidine-5'-monophosphate (dTMP). dTMP is a nucleotide required for DNA synthesis, and as such is an important potential drug target. In bacteria, deoxy-Uracil-5'triphosphate (dUTP) is formed first; either by the phosphorylation of deoxy-uracil-5'diphosphate (dUDP), or by the deamination of deoxycytidine triphosphate (dCTP) (Figure 5). dUTP is then converted to deoxyuracil monophosphate (dUMP) via dUTPase, and subsequently dTMP is formed by the action of Thymidylate synthase.

Thymidylate synthase catalyzes the conversion of 2'-deoxyuridine-5'monophosphate (dUMP) to thymidine-5'-monophosphate (dTMP) utilizing methylene-tetrahydrofolate (mTHF) as a methyl donor and reductant (Figure 4). Dihydrofolate (DHF) is a byproduct of this reaction, and goes on to be converted

to tetrahydrofolate by the enzyme Dihydrofolate reductase, and is ultimately converted back to mTHF by serine hydroxymythl-transferase. Even partial inhibition of ThyA's activity can lead to a buildup of 2'-deoxyuridine-5'-triphosphate, which in turns leads to a "thymine-less" cell death(21, 22).

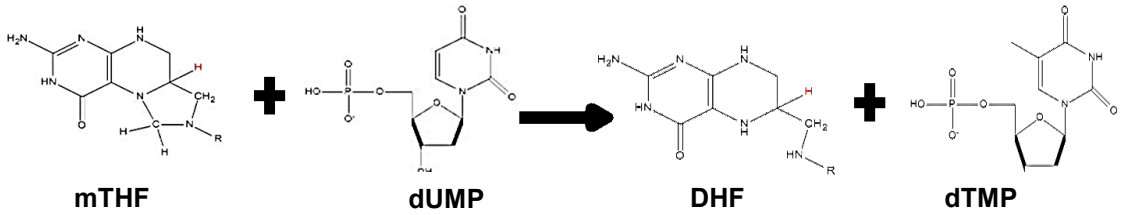

Figure 4- Thymidylate synthase reaction. ThyA catalyzes the conversion of 2'-deoxyuridine-5'monophosphate to thymidine-5'-monophosphate utilizing methylene-tetrahydrofolate as the methyl donor and reductant. DHF is a byproduct.

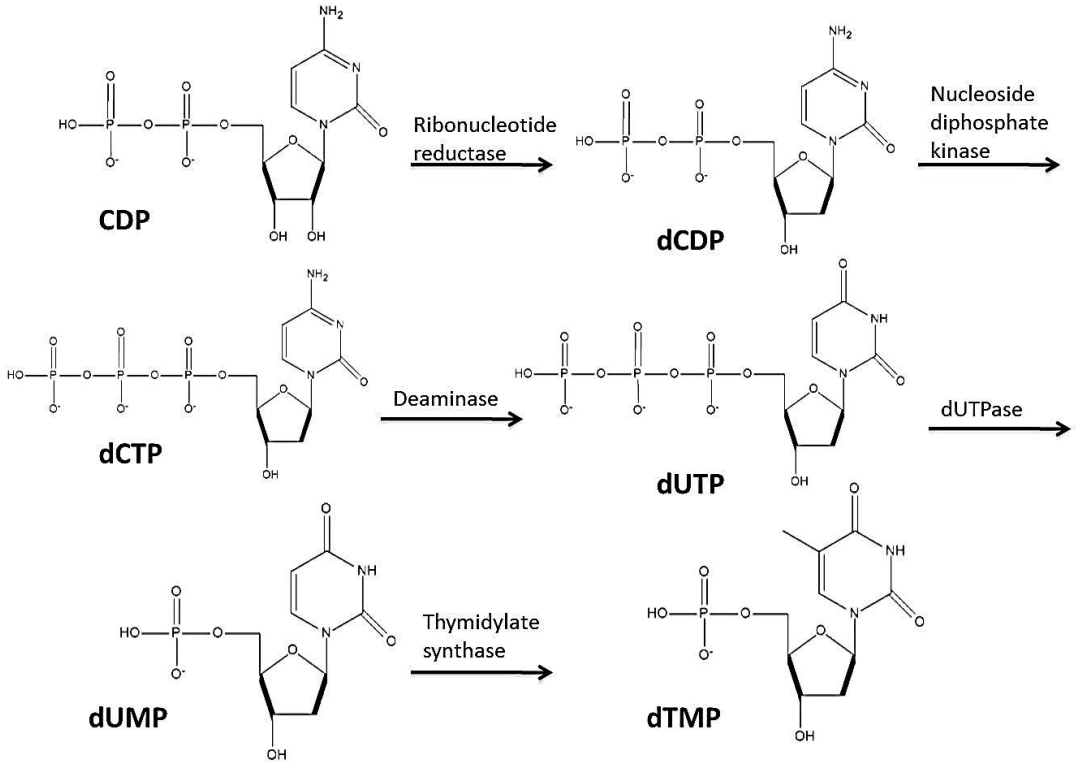

Figure 5- De novo TMP synthesis. The de novo pathway for TMP synthesis beginning with cytidine diphosphate. The pathway can also begin with uracil diphosphate being reduced and subsequently phosphorylated, at which point the two pathways converge

1.2.2 Mechanism of Thymidylate Synthase

The mechanism of Thymidylate synthase has been widely studied and is believed to be conserved across species. It has been validated by structures of reaction intermediate analogs with mechanism based inhibitors, and by site-directed mutagenesis (Figure 7) (13, 23-25). During the reaction, mTHF serves as both the one-carbon donor to the substrate, dUMP, as well as the reductant. The carbon and the hydride come from different sites on the cofactor. The reaction mechanism proceeds via an ordered Bi-Bi fashion, with dUMP binding to thymidylate synthase first (Figure 6).

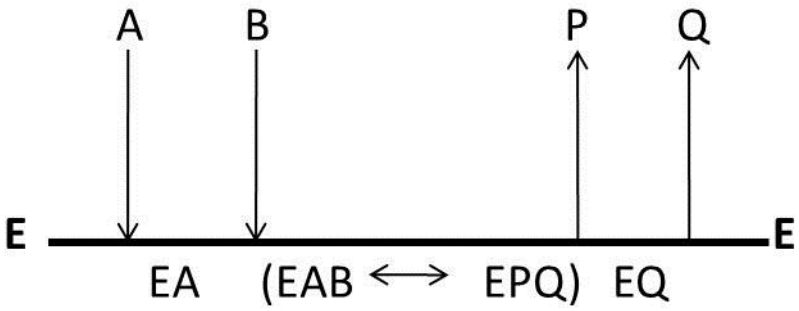

Figure 6- Bi-Bi Sequential Mechanism

Under conditions of saturating concentrations of mTHF, K_{cat}/K_m^{dUMP} is equal to the on-rate for dUMP (25). The binding of cofactor is more complicated, due to the fact that it involves association with the binary complex, ThyA-dUMP, closing of the active site, opening of the imidazolidine ring, and covalent bond formation with C5 of dUMP.

Catalysis begins by the nucleophilic attack of the active site Cysteine on C6 of dUMP, initiated by tight binding of the cofactor. Next is a 1,4-addition between the iminium ion (formed by opening of the mTHF ring) and C5 of dUMP, followed by abstraction of a proton from the C5 position of dUMP. β-elimination of the cofactor occurs next, and lastly the hydride transfer from mTHF to the methylene group at C5 of the pyrimidine. The reaction mechanism is depicted in Figure 7. The catalytic residues from *L. casei* were identified by site-directed mutagenesis, and of 25 conserved residues, five proved to be important for catalysis. In *L. casei*, these residues are Arg218 for dUMP binding, Asp221 for mTHF binding, Cys198 as the nucleophile attacking C6 of the pyrimidine, Tyr 146 for proton abstraction at the C5 position of dUMP, and Glu60 is involved in cofactor elimination from the covalent ternary complex(26).

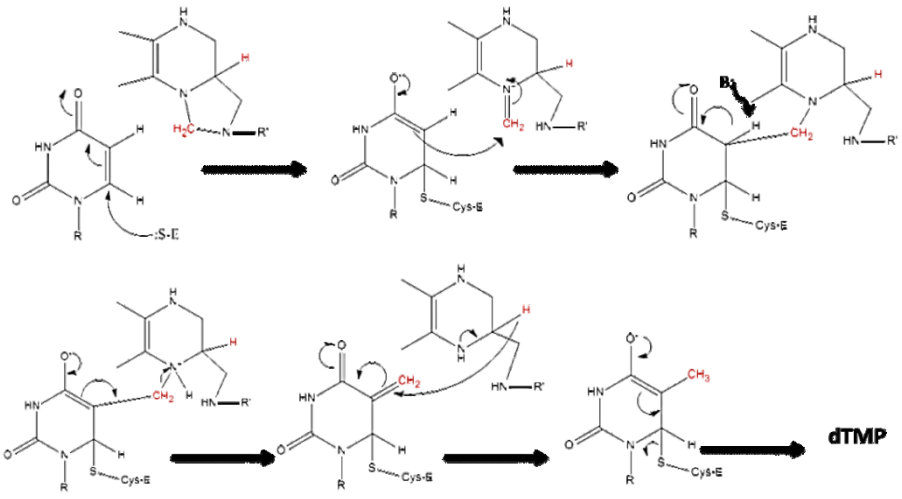

Figure 7- Reaction mechanism of thymidylate synthase. Validated by structures of reaction intermediate analogs with mechanism based inhibitors, and by site-directed mutagenesis.

1.2.3 Chemotherapeutics that target Thymidylate Synthase

1.2.3.1 Substrate analog FdUMP

5'-fluoro-2'-deoxyuridine-5'-monophosphate (FdUMP), the active metabolite of 5-fluorouracil (5-FU), competes with the natural substrate of thymidylate synthase, dUMP, to form a ternary complex with the enzyme (Figure 8). This complex does not dissociate easily and is deemed a dead-end inhibitor, since the fluoro group is located at the 5' position, where typically a hydrogen atom would be abstracted (21, 22, 27).

5-FU is commonly used to treat metastatic colorectal cancer, where the lack of dTMP, and buildup of dUMP, ultimately leads to the incorporation of deoxyuracil triphosphate into DNA. Other mechanisms of cytotoxicity include incorporation of FdUTP into DNA or FUTP into RNA. FdUTP incorporated into DNA during DNA synthesis leads to miscoding and eventually cell death (21).

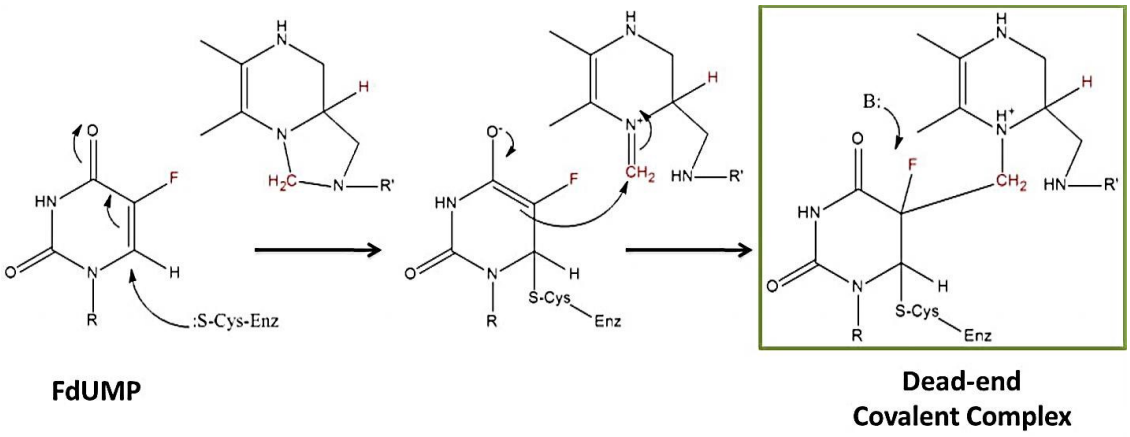

Figure 8- "Dead-end" inhibition of thymidylate synthase by FdUMP.

1.2.3.2 Pemetrexed

Pemetrexed is a pyrrolo[2,3-d]pyrimidine-based antifolate, which enters the cell and becomes polyglutamated by folypolyglutamate synthase (FPGS) (28). The main target is inhibition of thymidylate synthase, where it acts as an anti-folate, binding in the mTHF site of the enzyme. Inhibition of dydrofolate reductase and glycinamide ribonucleotide formyl transferase is also seen(29). In combination with 5-FU, Pemetrexed has a synergistic antitumor effect on tumor types including non-small cell lung, breast, colorectal, head and neck, gastric, bladder, cervix, and pancreas cancers(30-32). In human cancer cells, the K_i for monglutamated Pemetrexed is reported to be 100-fold weaker than the polyglutamated form, with K_i's of 109nM and 1.3nM, respectively.

1.2.3.3 Raltitrexed

Raltitrexed is another anti-folate that is rapidly taken up by the cell and is polyglutamated by FPGS. This polyglutamation leads to a 70-fold greater inhibition of thymidylate synthase, and has demonstrated activity in a variety of advanced solid tumors, such as colorectal and breast cancer (33-36). Furthermore, polyglutamation leads to a longer retention time in tumor cells, which reduces dosage, an option not possible with 5-FU. Raltitrexed is a ThyA specific inhibitor, unlike 5-FU which inhibits purine synthesis and has effects not only on DNA but RNA as well. This makes Raltitrexed less toxic, not leading to side-effects such as mucositis (37).

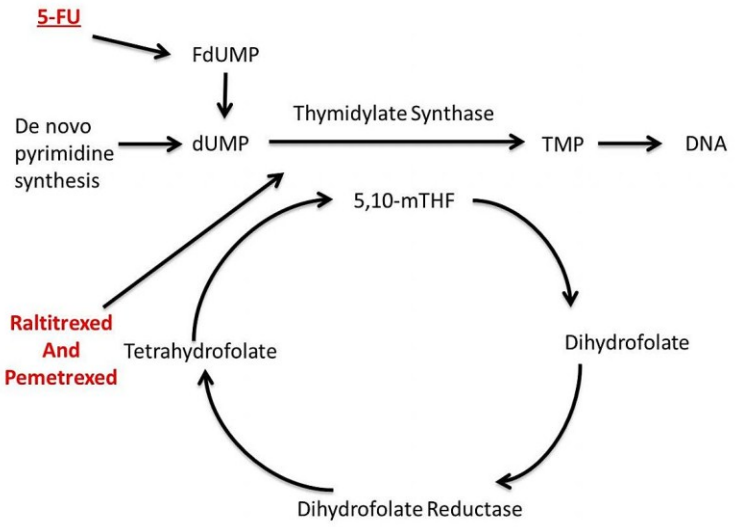

Figure 9- Downstream effect of inhibiting thymidylate synthase. Disruption of the folate cycle, as well as reduction in cellular TMP, ultimately leads to cell death.

2. STEADY STATE KINETICS AND INHIBITION OF Mtb ThyA

2.1 Introduction

Thymidylate synthase (TS) plays a crucial role in DNA biosynthesis and cell proliferation, and has therefore been the focus of extensive research as a drug target against cancer as well as infectious agents such as *M. tuberculosis*. In order to characterize its activity, several in vitro assays have been developed to determine the potential therapeutic effectiveness of anti-folates. The use of folate based inhibitors is believed to be less toxic than drugs that mimic dUMP, such as FdUMP, which may be inadvertently integrated into DNA or RNA(21).

Antifolate inhibitors are of special interest for another reason as well; it is often found that several enzymes may be the target of a single drug, which is the case with Pemetrexed where it has been shown to inhibit both TS as well as Dihydrofolate Reductace (DHFR)(28, 29). Thymidylate synthase inhibitors are generally characterized by the presence of a 2-substituted-4-oxo moiety in the pyrimidine, as seen in both Pemetrexed and Raltitrexed, whereas DHFR anti-folates will possess a 2,4-diamino in that position.

Due to the high degree of similarity between *M. tuberculosis* ThyA and other species, particularly in binding regions, the use of classical antifolates to combat tuberculosis may not prove to show enough discrimination between enzymes. For this reason, high throughput screening techniques to identify compounds that bind specifically to *Mtb* ThyA are an important tool for investigating species specificity. One such assay, fluorescence-based thermal

shift, utilizes the energetic coupling between ligand binding and protein unfolding to identify fragments that may have an affinity for the protein. The temperature at which a purified protein unfolds is measured by an increase in fluorescence of a dye, Sypro orange. As the protein unfolds, Sypro orange binds to the hydrophobic patches that become exposed, causing an increase in fluorescence (38-41). This allows the ability to assay a diverse set up compounds and potentially identify non-classical TS inhibitor candidates.

2.2 Experimental Procedures

Chemicals - 2′-Deoxyuridine 5′-monophosphate disodium salt, 5-Fluoro-2′-deoxyuridine 5′-monophosphate sodium salt, 2-mercaptoethanol, formaldehyde, and Raltitrexed monohydrate were all purchased from Sigma. (6R,S)-5,10-methylenetetrahydrofolate was purchased from Schircks Laboratories, Switzerland. Pemetrexed was purchased from LC Laboratories. The fragment library is from Maybridge.

Steady State and Inhibition Kinetics – The kinetic assay monitored the spectral change at 340nm attributed to mTHF being converted to DHF. The buffer for the assay contained 12mM formaldehyde, 100mM 2-Mercaptoethanol, 40mM Tris-Hcl pH 7.4, 20mM $MgCl_2$, 1mM dUMP, 0.75mM EDTA, 0.3mM (6R,S)-5,10-methylenetetrahydrofolate, and 400nM purified ThyA. The method was first described by Albert Wahba and Friedkin, and refined by Davisson et al. The reaction volume was 1.0mL and the absorbance measured in a Cary50 Spectrophotometer. A 1.5mM stock solution of mTHF was prepared in reaction

buffer, and 0.1M stock solutions of dUMP, FdUMP, Pemetrexed, and Raltitrexed were prepared in ultrapure water. All more dilute solutions were made from these. For the steady state kinetics, mTHF was held constant at final concentrations of 75uM, 150uM, 300uM and 600uM while the concentration of dUMP was varied at concentrations of 5uM, 10uM, 20uM, 32uM and 64uM. The reaction was initiated by the addition of 1 uL of 150uM thymidylate synthase, and the absorbance recorded over a three minute period at room temperature. Plots of reaction velocity versus substrate concentration were fit using KaleidaGraph, to the Michaelis-Menten equation for a sequential mechanism: $v=(V_{max}[A][B])/([A][B]+K_m^A[B]+K_m^B[A]+K_m^BK_s^A])$.

The assay was also used to determine IC_{50} and K_i values for the inhibitors by varying the substrate and corresponding inhibitor concentrations (concentrations of dUMP were varied against fixed concentrations of FdUMP, and concentrations of mTHF were varied against fixed Pemetrexed or Raltitrexed concentrations). The data yielded doubled reciprocal plots that were fit to linear regression lines. Plots of reaction rates versus substrate concentration were fit using KaleidaGraph to the appropriate Michaelis-Menton equation for inhibition by a non-competitive inhibitor, $v= (V_{max}[B])/ ((1+[I]/K_i)(Km^B+[B]))$, competitive inhibitor, $v= (V_{max}[B]/(K_m^B(1+[I]/K_i+[B]))$, or mixed inhibitor, $v= (V_{max}[B])/(K_s^A(1+[I]/K_i) + [B](1+[I]/K_{is}))$.

Differential Scanning Fluorimetry- Inhibitor compounds were screened using differential scanning fluoremetry in a 96-well Stratagene RT-PCR system.

ThyA enzyme, SYBR Orange, Magnesium Chloride, and HEPES pH 8.0 were combined with final concentrations of 6μM, 5X, 5mM, and 330mM, respectively; to a final volume of 19μL. 1μL of compound at 100mM was added and the solution thoroughly mixed. Controls substituted 1μL of 100mM dUMP or 1μL of water, to represent the substrate and apo forms of the enzyme, respectively. Temperature range scanned was 25°C to 75°C, with a 0.5°C increase per minute. Compounds were selected for further inhibition studies based on presenting a melting temperature equal to or greater than that of the dUMP bound enzyme.

2.3 Results

1. Steady State Kinetics of Mtb Thymidylate Synthase

Thymidylate synthase activity was determined using a direct spectrophotometric method, in which the oxidation of tetrahydrofolate was monitored at 340nm. To probe the order of substrate binding, the purified enzyme was assayed with increasing concentrations of either dUMP or mTHF, while varying the concentrations of the second substrate. Standard Michaelis-Menten curves were observed (Figure10). The reciprocal plots were also made and fitting of the data allowed the calculation of K_m values of 6 μM for dUMP and 60 μM for mTHF (Table 1).

The plots are consistent with an ordered sequential mechanism, with dUMP binding the enzyme first. *M. tuberculosis* ThyA has a very low turnover

rate, with an apparent K_{cat} value of only 4 min^{-1}. Limited need for TMP because of the slow growth of the bacteria may explain this.

Table1- Mycobacterium tuberculosis kinetic constants. Mtb values are compared with those reported for the *E. coli* and Human enzymes.
[a] Values reported by Appleman et al.
[b] K_m and K_{cat} values reported by Dev et al.
[c] K_i values reported by Kisliuk et al.

	K_m (μM)			K_i (nM)	K_i(μM)	K_i(μM)
Enzyme	**dUMP**	**mTHF**	**K_{cat} (min^{-1})**	**FdUMP**	**Pem**	**Ralt**
M.tb	5	60	4	2	16.8	3.2
E.coli [a]	1.2	13	1.9	-	76	5.7
Human [b,c]	2.5	12	150	1.7	9.5	0.38

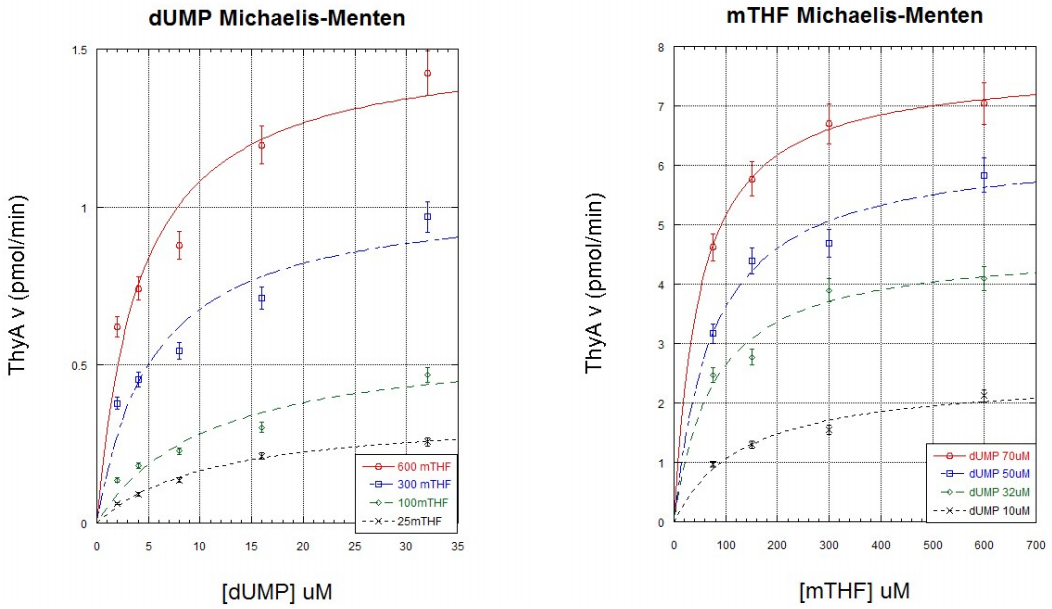

Figure 10- Michaelis-Menten Plots. (Left) dUMP is varied at fixed concentrations of mTHF (25μM, 100μM, 300μM, 600μM), (right) mTHF is varied at fixed concentration of dUMP (10μM, 32μM, 50μM, 70μM). Error bars are propagation of standard deviations.

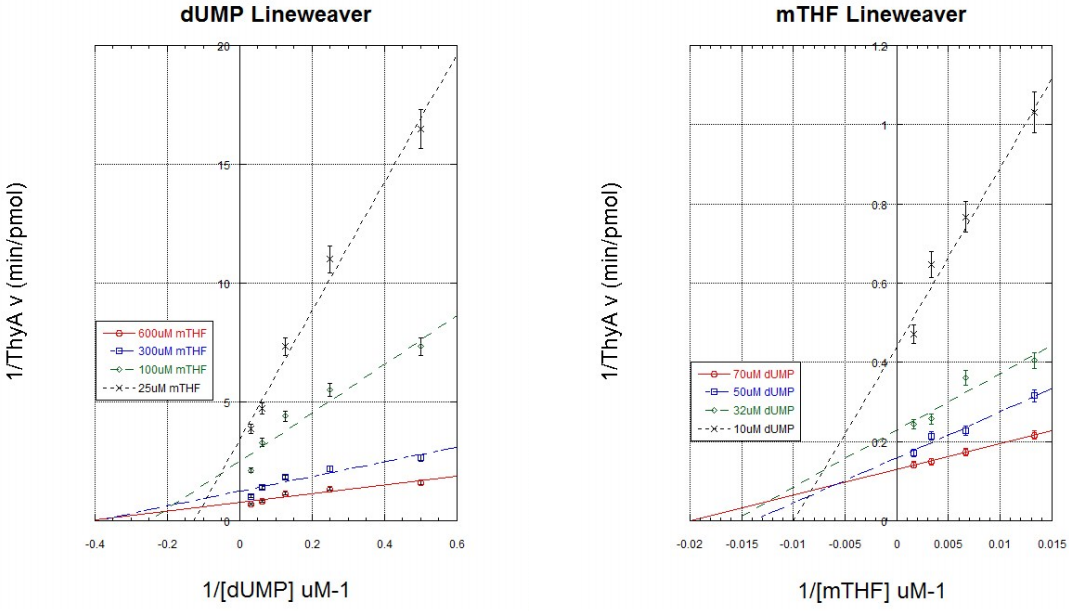

Figure 11- Double reciprocal plots of the data from Figure 10. Shows a sequential reaction mechanism. Error bars are propagation of standard deviations.

2. Inhibition of *M. tuberculosis* ThyA by Pemetrexed, Raltitrexed and FdUMP

FdUMP, the mechanism- based inhibitor, displayed low nanomolar range inhibition, with a K_i = 2nM. This is consistent with what has been reported previously (42). The substrate analog contains Fluorine at the 5' position of the pyrimidine ring, where typically hydrogen would be extracted during catalysis. The low nanomolar inhibition is the result of a dead-end covalent complex being formed between the catalytic cysteine of ThyA and the 5' C of the pyrimidine.

Raltitrexed and Pemetrexed, both chemotherapeutic anti-folates, were assayed in their monoglutamated form. Raltitrexed showed the best inhibition with a K_i= 3.2μM and an IC_{50} of 3.5μM, while Pemetrexed had a K_i= 16.8μM and an IC_{50} of 17μM. Compared to the human enzyme, K_i = 9.5μM for Pemetrexed, *Mtb* shows about 1.7 times weaker binding. For Raltitrexed, K_i=0.38 in huTS, the binding in *Mtb* is about 8.5 times weaker. Both Raltitrexed and Pemetrexed show tighter binding in *Mtb* ThyA versus *E. coli*, which has K_i values of 5.7μM and 76μM, respectively.

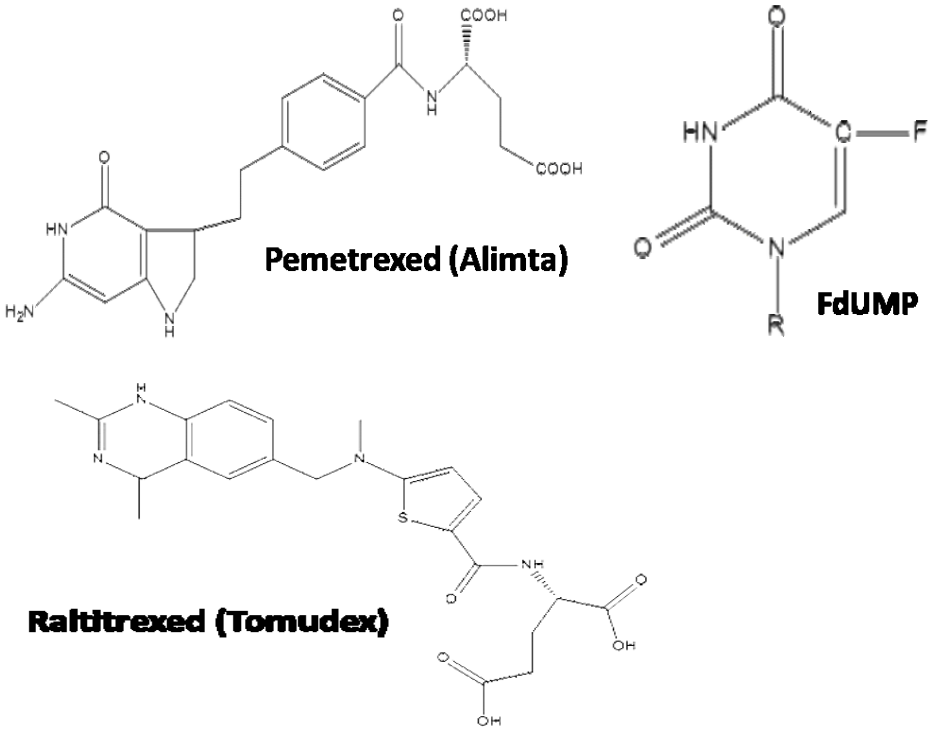

Figure 12- Pemetrexed, Raltitrexed, and FdUMP.

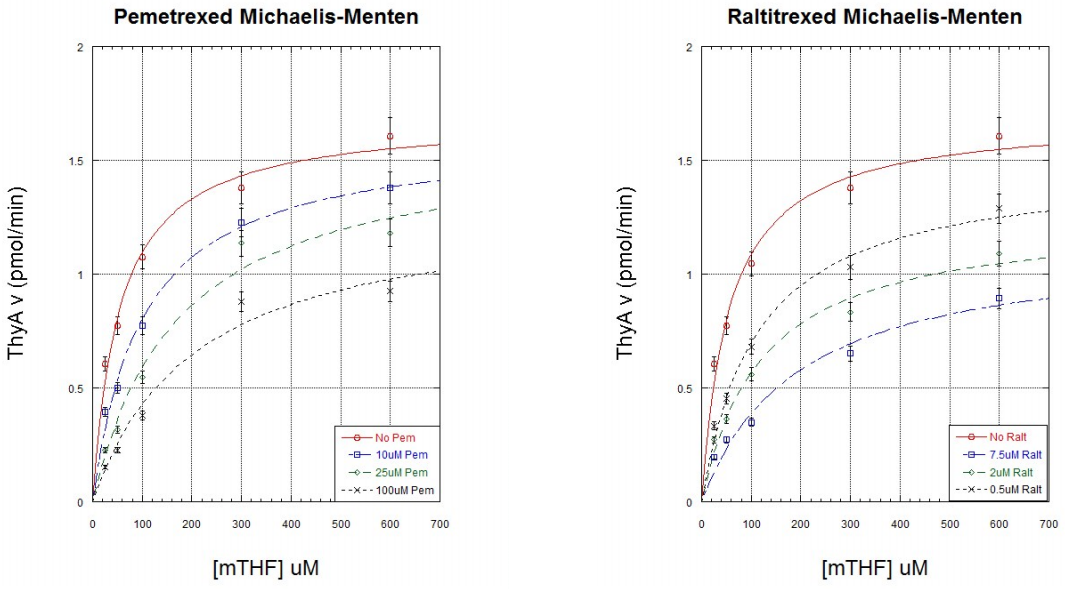

Figure 13 – Thymidylate synthase inhibition. (Top) Michaelis-Menten plots for ThyA inhibition by Pemetrexed and Raltitrexed. The concentration of dUMP was held constant at 100μM, and mTHF was varied at fixed concentrations of inhibitor. (Bottom) Double reciprocal plots, indicating noncompetitive inhibition for both drugs. Error bars are propagation of standard deviations.

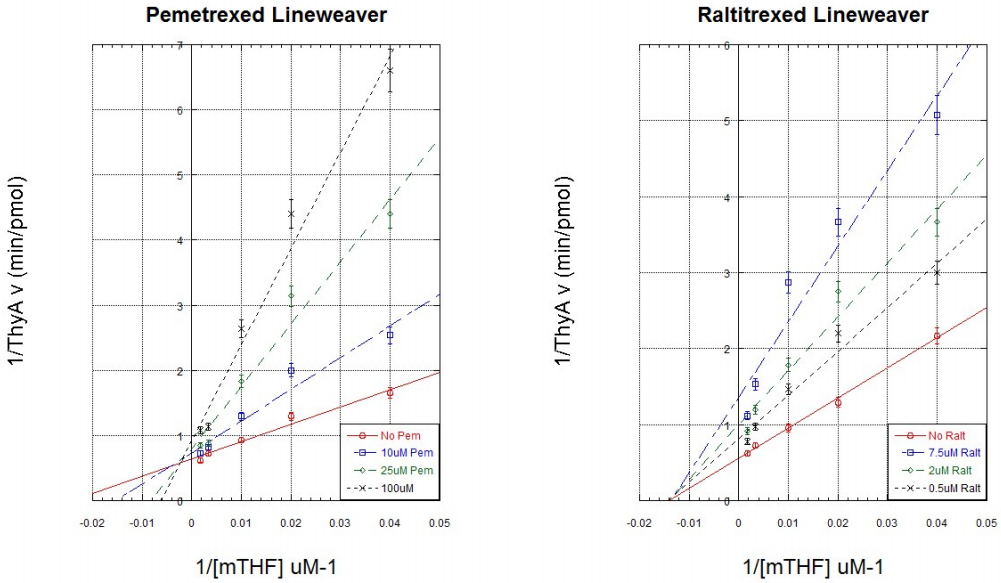

Figure 13 Continued.

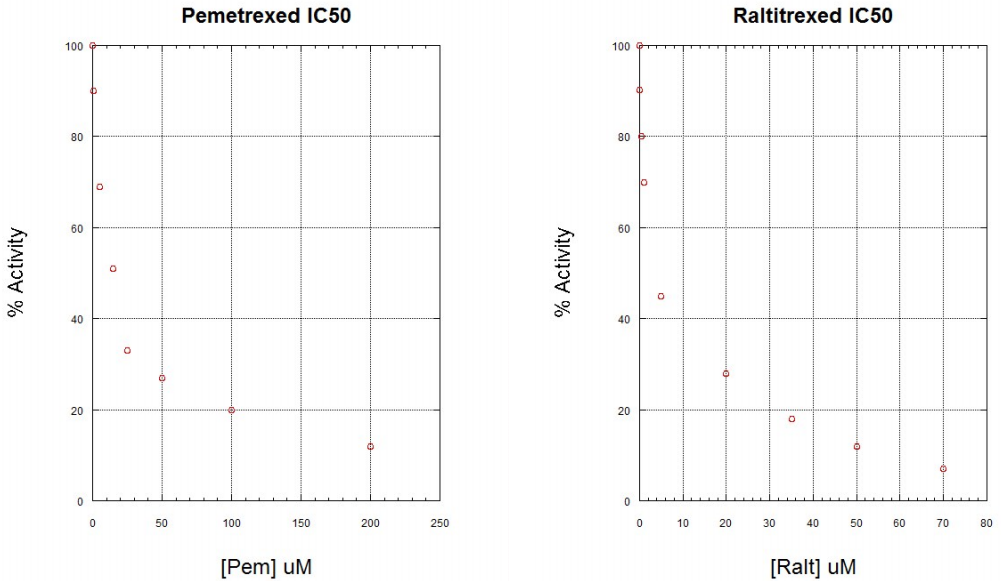

Figure 14- Inhibition curves for Pemetrexed and Raltitrexed. (Left) ThyA activity measured at increasing concentrations of Pemetrexed. The IC50 occurrs at 17μM. (Right) ThyA activity measured at increasing concentrations of Raltitrexed. The IC50 occurs at 3.5μM.

3. Identification of Lead Compounds by Differential Scanning Fluorimetry

The library of molecules screened consisted of 800 compounds with molecular weights of approximately 300 g/mole or less. Aside from the compound library, Pemetrexed, Raltitrexed, dUMP, and FdUMP were also screened to determine their effect on the melting temperature of apo ThyA, which melted at 41.5°C. The natural substrate, dUMP had a $\Delta T_{melting}$ of 6°C, while Pemetrexed gave a shift of 5°C; this was used as a lower threshold during the screening process.

After eliminating hits due to either non-reproducibility of shift or poor solubility, two compounds from the same plate remained; F9 and A7(Figure 15).

Of these two hits, F9 had the largest shift compared to the apo enzyme, with a $\Delta T_{melting}$ of approximately 9°C, while A7 showed a shift of 8°C.

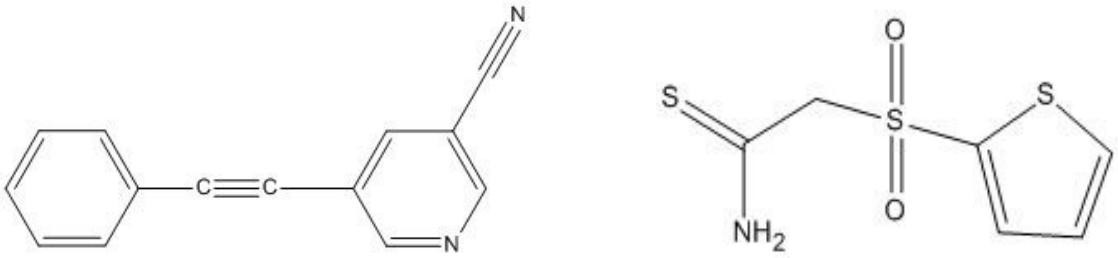

Figure 15 – Fragment Structures. (Left) Fragment F9, which displayed a change in melting temperature of 9°C versus apo ThyA. (Right) Fragment A7, which displayed a change in melting temperature of 8°C versus apo ThyA.

It is not possible to determine which binding site, if either, the fragments are bound to. It is also not believed that the degree of shift is necessarily correlated with a given level of inhibition; rather, the shift indicates that binding is occurring somewhere on the enzyme, and whether it is inhibitory or non-specific can only be determined through an X-ray structure. The use of this assay was not to identify a strong inhibitor; rather to identify lead compounds that in some cases may be linked or modified to form a more potent drug candidate. All efforts to crystallize ThyA bound with fragments F9 or A7 have not yet been successful, and additional fragment libraries are currently being screened.

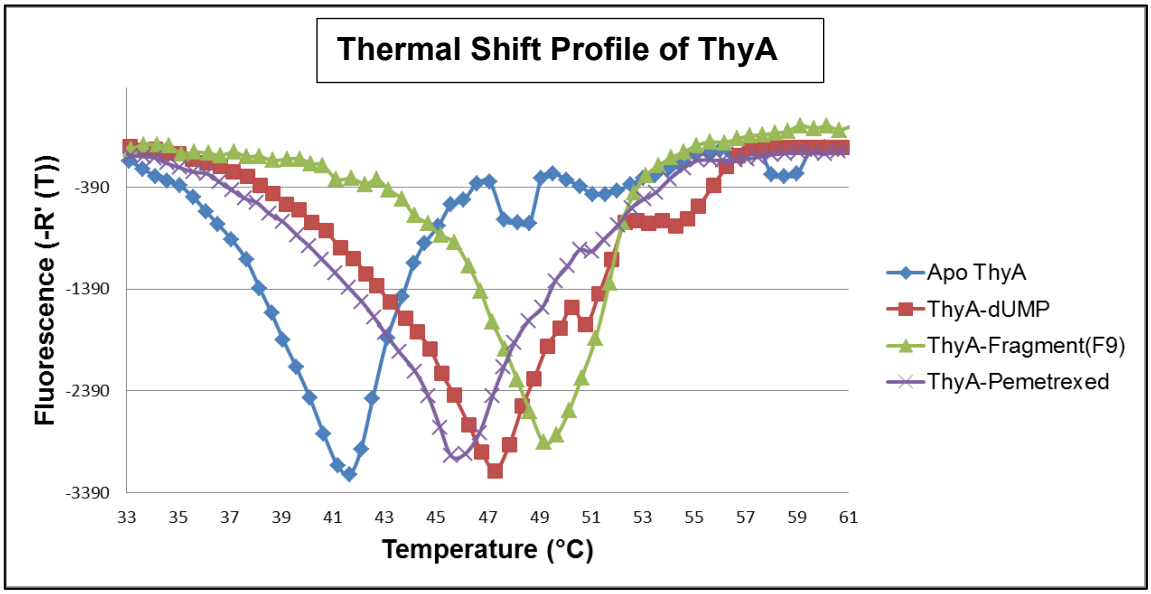

Figure 16- Thermal shift plot. Plot indicates the melting temperature of apo ThyA (blue), ThyA-dUMP (red), ThyA-FragmentF9 (green), and ThyA-Pemetrexed (purple).

2.4 Discussion

Inhibition of thymidylate synthase in human cancer cells with antifolates such as Pemetrexed and Raltitrexed, as well as with the dUMP analog FdUMP, is an avid area of research in recent years. Derivatives of the folate cycle are essential for cell growth and replication not only in eukaryotic cells, but in prokaryotic cells as well. Inhibition of TS also results in a depletion of the dTTP pool and an increase in dUTP. This results in a decrease in DNA synthesis and eventually cell death.

With this in mind, Raltitrexed and Pemetrexed were analyzed to determine their ability to inhibit *M. tuberculosis* thymidylate synthase. Each inhibited *Mtb* ThyA in the low micro molar range in vitro, and it is interesting to note that Pemetrexed inhibited the *Mtb* enzyme with a K_i of 16.8μM, which is a 4.5 fold greater affinity than what has previously been reported for *E.coli,* K_i = 76μM. Given the high degree of structural similarity and conservation of active site residues, this large of a difference in K_i was not immediately expected. Recent work by Costi et al. has shown the use of dansyl derivatives for the inhibition of *E.coli* and *L. casei*. N,O-didansyl-L-tyrosine (DDT) showed the tightest binding with a K_i of 1.8μM in *E.coli* and 1.4μM in *L. casei*, so was chosen to test its inhibition against Mtb ThyA. No inhibition was seen when tested at concentrations up to 100μM (work not shown). This result illustrates that small ligands have the ability to discriminate between highly conserved enzymes.

The use of differential scanning fluorimetry is an excellent means of exploiting such molecules and offers the ability to do so in a quick, easy to interpret fashion. Although confirmed hits of novel fragments have yet to be established in this study, the method was proven successful in so that a clear thermal shift was shown for substrate, dUMP, as well as the known anti folate Pemetrexed.

3. CRYSTAL STRUCTURES OF BINARY AND TERNARY COMPLEXES OF *M. tuberculosis* THYMIDYLATE SYNTHASE

3.1 Introduction

With the emergence of multidrug-resistant tuberculosis (MDR) and extensively drug-resistant TB (XDR), the need for novel therapeutics to combat this disease are greater than ever. The last first line drug to hit the market was Rifampin, and that was over 40 years ago. Treatment of MDR-TB requires a 24 month regimen of second line drugs, which is more costly, toxic, and less effective than first-line drugs. Even with over site by the World Health Organization to ensure proper use of second line TB drugs, it has still been reported that MDR TB strains have become resistant to these. The outcome of not developing a new first line anti-tubercular drug soon could be the outbreak of a very deadly, drug resistant strain of TB.

Thymidylate synthase has been much studied as its role as a chemotherapeutic agent, as well as its potential as an anti-microbial. Crystal structures of ThyA from *E. coli*, *Cryptococcus neoformans*, *Lactobacillus casei*, and human have all been solved and show high levels of conservation in the overall fold of the enzyme, as well as in catalytic residues. Variations in K_i of known inhibitors, though, lead to the conclusion that bacterial or species specific thymidylate synthase drugs are possible. A thorough understanding of the structure of *Mycobacterium tuberculosis* thymidylate synthase opens the door to being able to design such a drug.

Furthermore, mycobacterium lacks the gene encoding Thymidine Kinase, which in most organisms catalyzes the conversion of thymidine to dTMP *via* a phosphate transfer from ATP. This underscores the significance and essentiality of *de novo* TMP synthesis in this organism.

3.2 Experimental Procedures

Chemicals- 2′-Deoxyuridine 5′-monophosphate disodium salt, 5-Fluoro-2′-deoxyuridine 5′-monophosphate sodium salt, and Raltitrexed monohydrate were all purchased from Sigma. Pemetrexed was purchased from LC Laboratories.

Cloning, Expression and Purification – The ThyA gene, Rv2764c from *M. tuberculosis* H37Rv genome, was identified from TubercuList sequence data base. The ThyA gene was amplified using *M. tuberculosis* genomic DNA as a template and cloned into a pET28b expression vector (Novagen) with an N-terminal His tag. The vector was transformed into *Escherichia coli* overexpression strain, BL21(DE3). Cells were grown at 37^{o}C until they reached an optical density of 0.6, and then induced with 1mM isopropyl-1-thio-β-D-galactopyranoside. The temperature was then reduced to 18 ^{o}C for 24 hours. The cells were spun and pellets re-suspended in 20mM Tris-HCl pH 7.0 containing 100mM NaCl and 10mM imidazole. The cell extract was applied to a 5-mL nickel-nitrilotriacetic acid column (GE Lifesciences), and the target protein was eluted using an imidazole gradient. ThyA eluted at approximately 100mM imidazole. The eluted protein was dialyzed overnight against 4 liters of 20mM

Tris-HCl pH 7.0, containing 100mM NaCl, 10% glycerol, and 1mM DTT. The protein was then concentrated with Amicon 10K concentrating tubes to a final concentration of 15mg/mL. The final protein was greater than 95% pure as seen on an SDS-PAGE gel.

Crystallization – The initial crystallization condition was obtained using Wizard II from Emerald BioSystems. Crystals were grown using the hanging drop vapor diffusion method at 16^{o}C. Crystals of the binary complexes, ThyA-dUMP and ThyA-FdUMP, were obtained by incubating 15mg/mL of purified thyA with 3mM of the respective compound along with 1mM spermidine tetrahydrochloride for a period of two hours. Crystals of the ternary complex, ThyA-dUMP-Pemetrexed, were obtained by incubating with 3mM of dUMP, 3mM Pemetrexed, and 1mM spermidine tetrahydrochloride for 2 hours. In both cases, 3 uL of incubated 15 mg/mL protein was added to 2uL of reservoir buffer containing 0.1M Tris pH 7.0, 0.2M NaCl, and 30% (w/v) PEG-3000. Crystals appeared within 24-48 hours.

Data Collection and Processing- High resolution data was collected at beamlines 19id and 23id at the Advanced Photon Source, Argonne National Laboratory. All data was indexed and scaled using HKL2006. Unit cell dimensions for dUMP bound crystals were a = 184.9, b = 84.9, c = 130.1 α = 90.0, β = 107.9, γ = 90.0; for fdUMP crystals they were a = 184.3, b = 82.3, c = 125.9 α = 90.0, β = 131.0, γ = 90.0; for Pemetrexed- dUMP bound crystals they were a = 100.1, b = 57.0, c = 113.7 α = 90.0, β = 107.9, γ = 90.0. All crystals

were space group C2; however, the Pemetrexed-dUMP ternary complex consisted of 2 molecules in the asymmetric unit, while dUMP and FdUMP binary complexes each displayed 4 molecules in the asymmetric unit.

Structure Determination of Substrate Bound Thymidylate Synthase - The dUMP bound structure of *Mtb* thymidylate synthase was solved by molecular replacement using MolRep of the CCP4 suite of programs. Molecular replacement uses the phases from structure factors of a known protein as initial estimates of phases for a new protein. The known protein is the phasing model, which in this case was from *Escherichia coli* Thymidylate synthase (PDB 2FTQ). This method calculates initial phases by placing a model of the known protein (*E.coli* ThyA), in the asymmetric unit of the new protein (*Mtb* ThyA). The search is broken up into two parts: rotational and translational. In the rotational search, the orientation of the molecules is determined by the match of intramolecular Patterson vectors. The intramolecular Patterson vectors are used (distances between ~10-4Å) because they are indicative of the relative locations of secondary structure elements, whereas very large distances will contain intermolecular vectors, which differ for each packing situation and may not be useful. Correlation coefficients were calculated for each rotation of the Patterson map over all angles. The orientation giving the highest correlation coefficient was chosen as the best orientation for the phasing model.

Next, in the translation search, the criterion is the correspondence between the expected structure-factor amplitudes from the model in a given trial

location and the actual amplitudes derived from the native data on the desired protein. The R-factor is monitored which compares the overall agreement between the amplitudes of two sets of structure factors. A small R-factor indicates that the observed and calculated intensities agree with each other. A solution was found and refinement was done by rigid body and restrained refinement, using RefMac5, followed by simulated annealing using Phenix refine, and another round of restrained refinement. The substrate dUMP was made using PRODRG and fit to the electron density map using Coot. Several rounds of manual refinement were performed. The model was subjected to another round of refinement in RefMac and solvent molecules were added before a final round of refinement was performed. The R_{work} and R_{free} values were 0.16 and 0.21, respectively.

Structure Determination of Inhibitor Bound Thymidylate Synthase- Inhibitor bound *Mtb* thymidylate synthase crystals, containing either bound FdUMP in a binary complex or dUMP-Pemetrexed in a ternary complex, were solved by molecular replacement with the solved *Mtb* thymidylate synthase-UMP bound structure as a search model. Water molecules and dUMP were removed from the structure prior to molecular replacement. Refinement was carried out using RefMac5 and ligands fit to the electron density in Coot. After final refinement, the R factors for the FdUMP structure were 0.21 and 0.26 and the R factors for the dUMP-Pemetrexed structure were 0.15 and 0.19.

3.3 Results

1. Crystal Structures of *M. tuberculosis* ThyA Binary Complexes, ThyA-dUMP and ThyA-FdUMP

The x-ray structure of the recombinant *Mtb* ThyA-dUMP binary complex was solved from electron density maps calculated by molecular replacement with *Escherichia coli* Thymidylate synthase. The crystals grew after incubation of the protein with dUMP, and the space group of the crystals was found to be C2. The structure has been refined to an R_{work} of 0.16 and an R_{free} of 0.21. The monomeric subunit of *Mtb* thymidylate synthase has 83% identity with the previously solved structure from *E. coli*. The monomeric unit folds into three domains consisting of a large six-stranded mixed β-sheet surrounded by α-helices (Figure 17). A total of 23% of the enzyme is comprised of β-sheets, including the dimer interface which is a β-sandwich. The asymmetric unit was comprised of two dimers, being stabilized at the dimer interface with a spermine molecule, which was used as an additive during crystallization.

The FdUMP binary complex was solved from electron density maps calculated by molecular replacement with the *Mtb* ThyA-dUMP structure, with calculated R_{work} and Rf_{ree} values of 0.21 and 0.26 respectively. The asymmetric unit was comprised of a single biological dimer. The overall structure of the ThyA-FdUMP complex is identical with that of the dUMP bound enzyme, with one exception. In the FdUMP structure, the fluorine atom makes hydrogen bonding interactions with a conserved water molecule as well as with the OH

group of Tyr94 (Figure 18). In both structures, the nucleotide binds to the open conformation of the enzyme, in position to make a covalent adduct between C-6 of the pyrimidine ring, and Cys146 upon binding of cofactor.

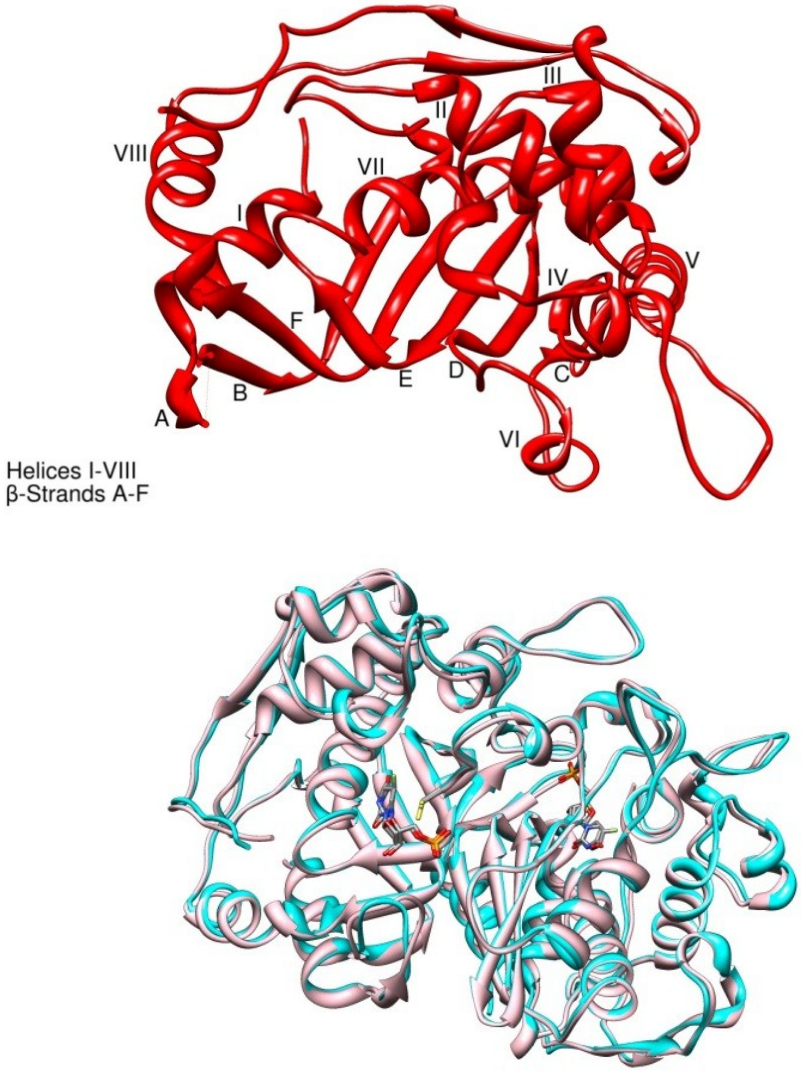

Figure 17- ThyA Domains and ThyA-dUMP/ThyA-FdUMP Superposition. (Top) Monomer of Mycobacterium TS with Helices and β-strands indicated. (Bottom) Superposition of ThyA-dUMP and ThyA-FdUMP complexes

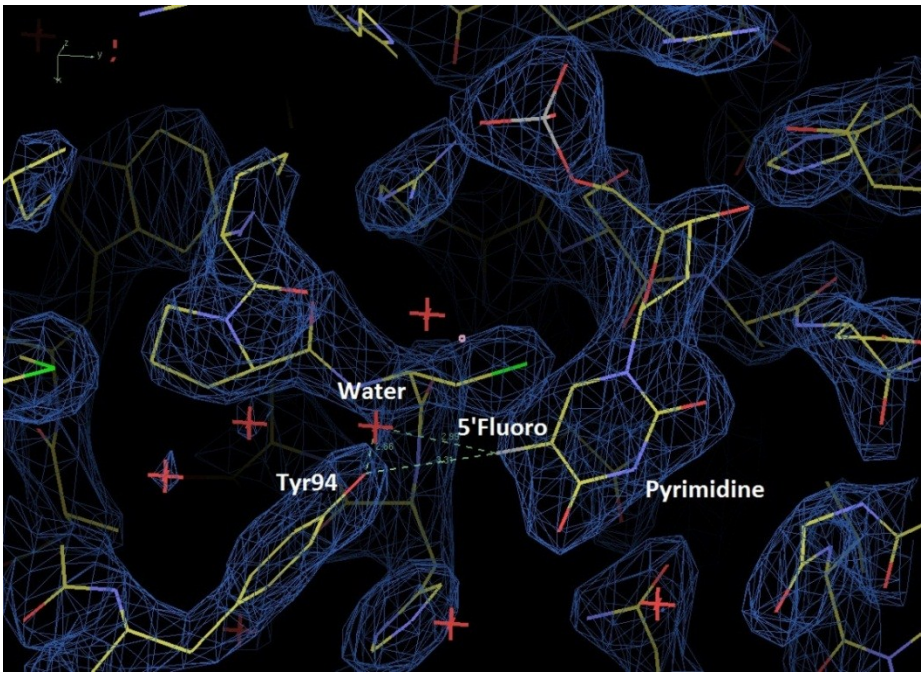

Figure 18- FdUMP Electron Density (Active Site). Electron density map showing the interaction of the 5'fluoro group with bridging Hydrogen bonds between Tyr94 and an active site water molecule. This interaction can't be made in the dUMP bound

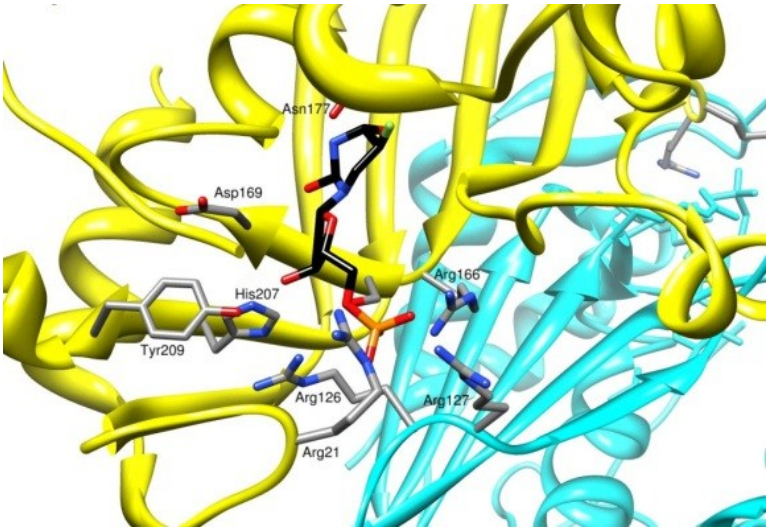

Figure 19- dUMP/FdUMP superposition of active site binding. Arg126 and Arg127 are from the opposing monomer. Five interactions stabilize the 5'Phosphate.

Table2- Data Collection and Refinement Statistics

	Pemetrexed	dUMP	FdUMP
Resolution	22.3-1.7	32.0-2.5	42.9-2.4
# Reflections			
Working Set	52863	49396	50786
Test Set	2775	2659	2712
R_{crys}	0.15	0.16	0.21
R_{free}	0.19	0.21	0.26
Average B	21.4 $Å^2$	46 $Å^2$	44 $Å^2$
Rms from ideal			
Bond Length(Å)	0.005	0.007	0.008
Bond Angle (^{o})	0.74	1.13	1.15

It has been shown by Lew et al., that in the absence of mTHF, FdUMP is at equilibrium with its covalent and non-covalent form. The presence of a folate shifts this equilibrium towards covalent adduct formation. This is consistent with

the binary structure of *Mtb* ThyA-FdUMP, in that no covalent adduct in observed. Stability of both dUMP and FdUMP is provided through several conserved hydrogen bonding interactions: the 2-oxo group of the pyrimidine with the backbone amide of Asp169, the N-3 of the pyrimidine and the Fluorine with Asn177, the 3'Hydroxyl with His207 and Tyr209, and the 5'Phosphate makes five interactions with Arg21, Arg126-127 of the opposing monomer, Arg166, and Ser167 (Figure 19). The five hydrogen bonding interactions with the phosphate tail of dUMP may account for the fact that 2'-deoxyuridine is not a substrate for ThyA (Reyes&Heidelberger, 1965). Hydrophobic contacts made by the pyrimidine include side-chains of residues Trp80, Tyr94, Leu143, Cys146, His147, Gln165, Ser167, and main chains of residues Ser167, Cys168, and Gly173. The ribose of dUMP/FdUMP makes hydrophobic interactions with the side chains of Leu143, Tyr209, Arg126, and the main chain and side chain of Asp169. Data collection and refinement statistic for all structures can be seen in Table 2.

2. Ternary Structure of *Mtb* ThyA-dUMP-Pemetrexed

The x-ray structure of the recombinant ternary complex, *Mtb* ThyA-dUMP-Pemetrexed, was solved from electron density maps calculated by molecular replacement with the solved *Mtb* TS-dUMP structure. The final model has R_{work} and R_{free} values of 0.15 and 0.19, respectively, and a space group of C2 with a full physiological dimer in the asymmetric unit (Figure 20).

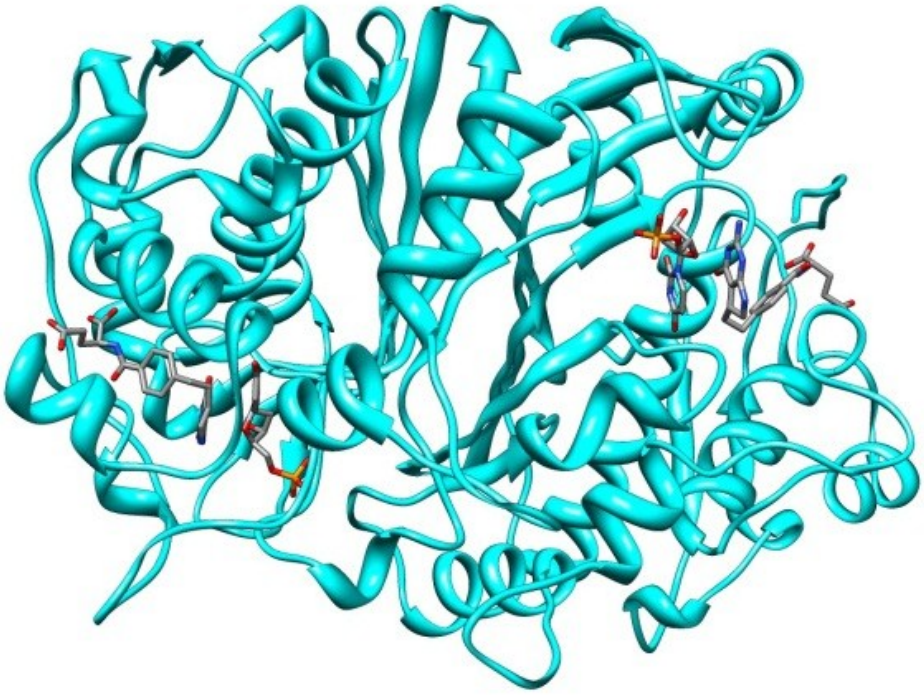

Figure 20- ThyA dimer with bound dUMP and Pemetrexed.

Pemetrexed was found to be bound in the active site of each monomer, with the fused ring system of Pemetrexed centered over the dUMP pyrimidine, causing planar ring stacking interactions which orient the inhibitor (Figure 21). No covalent bond was found between the C6 of dUMP and Cys146 after refinement, with a separation of 2.51Å. This is in contrast to what is seen in the EcTS crystal structure with the polyglutamated Pemetrexed, where a covalent adduct is seen to form in both binding pockets. Polyglutamation may lead to an

alternate conformation of Pemetrexed, which forces dUMP into the non-productive covalent complex.

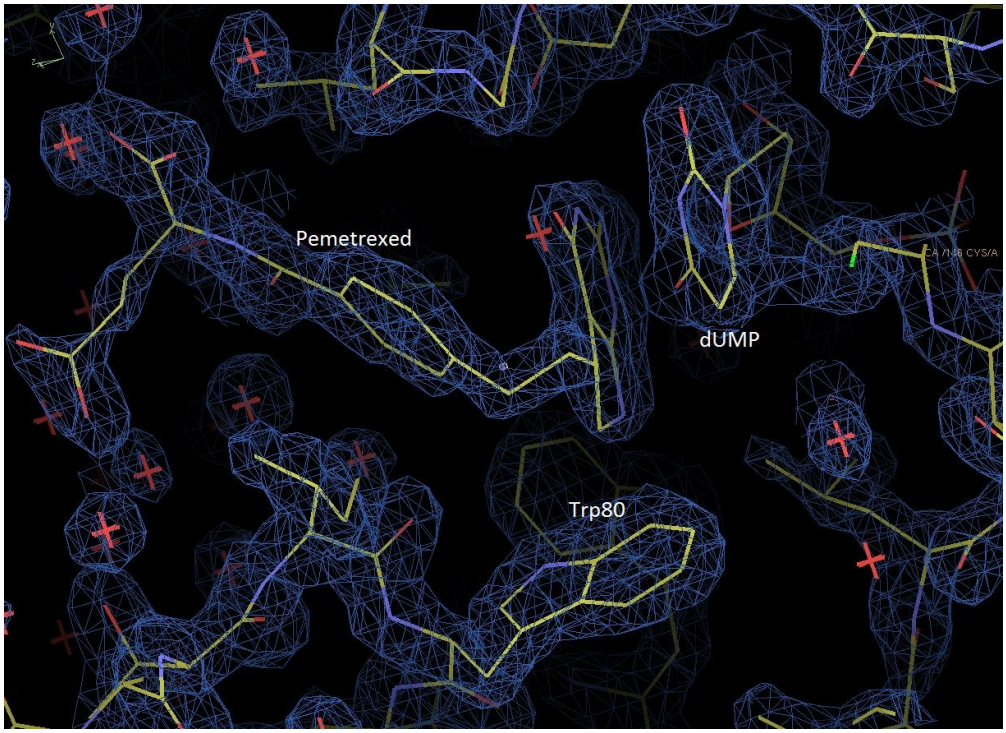

Figure 21- ThyA active site with bound dUMP/Pemetrexed. The fused ring system of Pemetrexed centers over the dUMP pyrimidine, causing planar ring stacking interactions which orient the inhibitor

The interactions made by the ring system of Pemetrexed parallel those made by the human thymidylate synthase, with two key differences. In human TS, Met311 is involved in a hydrophobic interaction with the ring system, which cannot occur in *Mtb* ThyA because this residue is a Valine. Also, human ThyA has an Asn which acts as a hydrogen bond acceptor from the N7 of the pyrrolo

ring of Pemetrexed; this residue in *Mtb* ThyA is a Trp. Pemetrexed is located in the folate binding site cushioned by five main hydrophobic interactions; Ile79, Trp80, Trp83, Leu172, and Phe176 (Figure 23). Pemetrexed includes an exocyclic amino group at the 2-position of the pyrrolo ring, which forms a hydrogen bond interaction with the backbone carbonyl of Ala262. There is also a conserved water molecule that mediates hydrogen bonding between the same amino group of Pemetrexed, the δ^2-O of Asp169, and the protein backbone at Ala262.

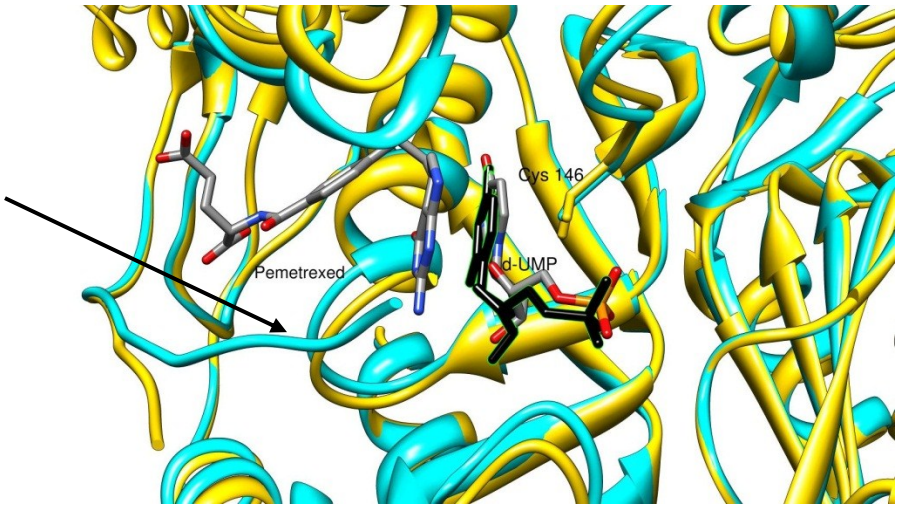

Figure 22- Superposition of ThyA-dUMP binary complex (gold) with ThyA-dUMP-Pemetrexed ternary complex (cyan). Shows closure of the active site upon binding of Pemetrexed (arrow).

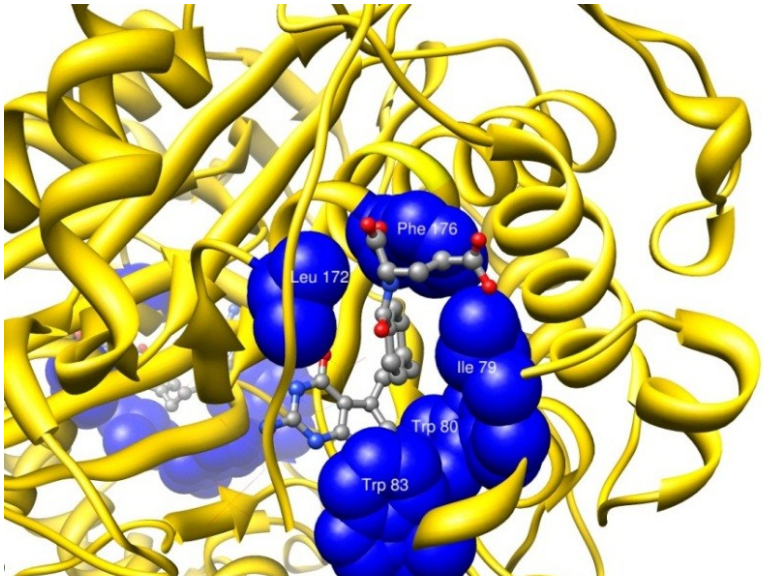

Figure 23- Pemetrexed hydrophobic interactions. Pemetrexed is located in the folate binding site cushioned by five main hydrophobic interactions; Ile79, Trp80, Trp83, Leu172, and Phe176

3.4 Discussion

M. tuberculosis thymidylate synthase is an obligate homodimer, and contains one active site per subunit. Each active site consists of catalytic residues from each monomer, meaning that a single subunit on its own would not be active. The binding pocket and catalytic residues are highly conserved across species. The residues involved in ligand binding and catalysis for *Mtb* ThyA have been identified as follows: Arg166 for dUMP binding, Asp169 for mTHF or anti-folate binding, Cys146 as the nucleophile attacking C6 of the pyrimidine, Tyr-94 for proton abstraction at the C5 position of dUMP, and Glu58 is believed to be involved in cofactor elimination from the covalent ternary complex.

This study reports the first crystal structures of *Mycobacterium tuberculosis* thymidylate synthase, which provides valuable structural insight into the binding of substrate and inhibitors to *Mtb*. It also allowed for the comparison of *Mtb* ThyA and other thymidylate synthases. In ternary complex with Pemetrexed and dUMP, *Mtb* ThyA fails to form a covalent adduct with the substrate, and the K_i of 16.8μM is almost 2-fold weaker than that of huTS, K_i = 9.5μM, where a covalent bond is evident in the crystal structure. Coupled with the inability to form a hydrogen bond at the N7 position of the Pemetrexed pyrrolo ring, this may explain the weakened affinity of the mycobacterium TS. In both *Mtb* and human structures, binding of Pemetrexed causes an ordering of the C-terminus of the enzyme, resulting in a closure of the active site cavity (Figure 21). In the case of substrate and cofactor, this would block the active site from solvent molecules and allow for catalysis to proceed. Aside from the active site, *M. tuberculosis* TS differs from the human TS by the conversion of a cysteine in the human enzyme to a serine in the mycobacterium. This residue is located on the beta sheet that forms the dimer interface. In the human enzyme, the cysteine allows thymidylate synthase to bind its mRNA and regulate its own translation. This suggests that *Mtb* ThyA expression levels may be dominated by regulation of RNA transcription, rather than autologous translational feedback loops.

Despite the fact that the crystal structure of the ternary complex ThyA-dUMP-Raltitrexed has not been fully solved (still in refinement), the kinetics

indicate that *in vitro*, Raltitrexed has a K_i of 3.2μM, which makes it about a 5 fold better inhibitor than Pemetrexed; both in their mono-glutamated form. This may even increase substantially in vivo upon polyglutamation, and whole cell assays should be performed on each.

This lab is continuing to work on solving crystal structures of *Mtb* ThyA in complex with known anti-folates, as well as lead compounds identified through fluorescence-based thermal shift assays. Solving of the apo structure is also of interest because it would help in understanding the overall mechanics of active site closure and what rearrangements take place upon dUMP binding. Furthermore, product bound crystals are of interest to understand what changes regulate release of DHF and dTMP after catalysis. Currently, crystals of ThyA-dTMP-Pemetrexed have been grown, and work is being done to crystalize the ternary complex ThyA-FdUMP-DHF. Together, these may give the insight necessary to answer these questions.

4. SUMMARY

Tuberculosis is currently treated with a plethora of first and second line antibiotics. Two of these drugs, Isoniazid and Ethambutol, target different areas of the bacterial cell wall. Isoniazid is the synthesis of mycolic acid, while Ethambutol inhibits arabinogalactan synthesis. The most recently introduced drug, Rifampicin, inhibits the beta-subunit of the RNA polymerase of prokaryotes. Despite therapeutic regimens containing combinations of these drugs, multi-drug resistant and extensively drug resistant strains of *Mycobacterium tuberculosis*, the causative agent of TB, continue to arise.

Thymidylate synthase has proven to be an important target in the treatment of many types of cancer including non-small cell lung, breast, colorectal, head and neck, gastric, bladder, cervix, and pancreas cancers. ThyA plays a crucial role in cell proliferation *via* production of TMP, and also through its role in the folate cycle (Figure 24). Folate deficiency inhibits cellular proliferation, disturbs cell cycling, causes genetic damage, and eventually results in cell death (43-45).

Raltitrexed and Pemetrexed are both antifolates that enter cancer cells via the reduced folate carrier as well as the α-folate receptor, which is overexpressed in some epithelial tumors (46). Once in the cell, Raltitrexed and Pemetrexed become polyglutamated by folylpolyglutamyl synthase, which increases the size and ionization state of the molecule. This decreases cellular

efflux, which leaves the drugs trapped in the cell for longer periods of time to act on their target, ThyA.

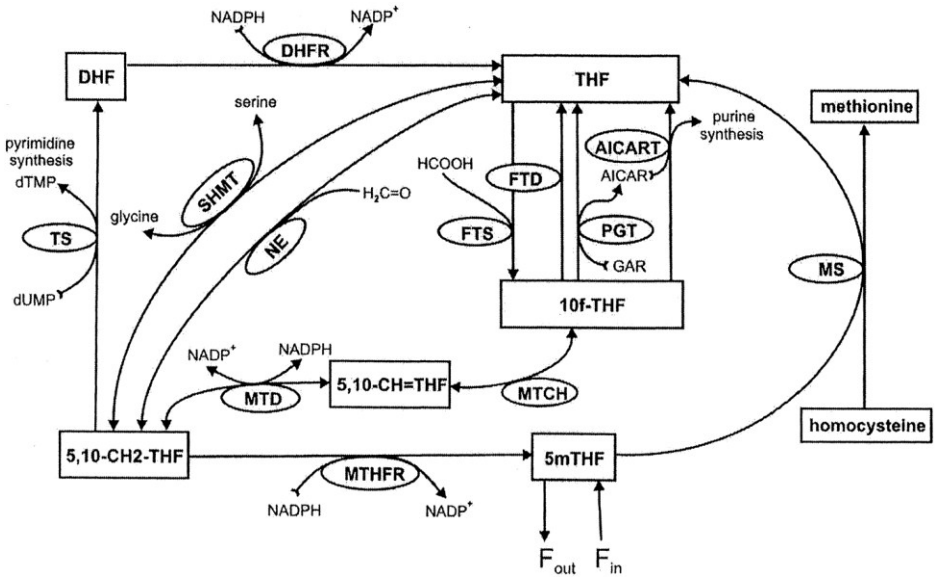

Figure 24- Folate cycle. Folate deficiency inhibits cellular proliferation, disturbs cell cycling, causes genetic damage, and eventually results in cell death.

Thymidylate synthase is an essential enzyme in the survival of *Mycobacterium tuberculosis*, therefore it's potential as a drug target in fighting this disease as well, has been explored. Pemetrexed and Raltitrexed in their monoglutamated forms have been shown in this study to have in vitro activity in the low micro molar range. This leads to the hypothesis that in vivo activity will be much greater, assuming transport into the cell and polyglutamation.

Given that mycobacterium lacks Thymidine Kinase, it may prove that antifolate inhibition of ThyA does not have to be species specific in fighting tuberculosis. Given the rate of success in treating colorectal cancer with Raltitrexed, and pancreas, bladder, and cervical cancer with Pemetrexed, similar results might be observed if Raltitrexed or Pemetrexed are used to treat *Mtb*.

In vivo experiments to determine the toxicity of these two drugs on *Mycobacterium tuberculosis* would define the extent to which polyglutamation increases their effectiveness, as well as determine whether there is transport of the drug into the bacterial cell. The design of a lipophilic anti-folate may be necessary, but utilizing the crystal structure of bound Pemetrexed as a scaffold, the design of a novel antifolate to fight *Mtb* is possible.

The crystal structures presented here open the door to the specific design of *Mycobacteria*l antibiotics. However, considering the homology with human thymidylate synthase, it is prominent that the design of anti folates of a dual nature (anti-cancer/anti-bacterial) is also possible.

REFERENCES

1. Davies PD. Tuberculosis: the global epidemic. J Indian Med Assoc. 2000;98:100-2.

2. Keeler E, Perkins MD, Small P, Hanson C, Reed S, Cunningham J, et al. Reducing the global burden of tuberculosis: the contribution of improved diagnostics. Nature. 2006;444 Suppl 1:49-57.

3. Migliori GB, Centis R, Lange C, Richardson MD, Sotgiu G. Emerging epidemic of drug-resistant tuberculosis in Europe, Russia, China, South America and Asia: current status and global perspectives. Curr Opin Pulm Med. 2010;16:171-9.

4. Shah NS, Wright A, Bai GH, Barrera L, Boulahbal F, Martin-Casabona N, et al. Worldwide emergence of extensively drug-resistant tuberculosis. Emerg Infect Dis. 2007;13:380-7.

5. Marshall E. Trench warfare in a battle with TB. Science. 2008;321:362-4.

6. Sharma M, Khayyam, K, Alam, S, Iqbal, M, Anwer, M, Imam, F. Tuberculosis: Brief overview and its shifting paradigm for management in India. International Journal of Pharmacology. 2010;6:755-83.

7. Tayler EM. Mantoux screening for tuberculosis. Lancet. 1995;345:930-1.

8. Samaria JK, Matah SC. Mantoux test and its relevance in the diagnosis of adult tuberculosis disease. J Assoc Physicians India. 1994;42:666, 9.

9. Aziz S, Haq G. The Mantoux reaction in pulmonary tuberculosis. Tubercle. 1985;66:133-6.

10. Venkataraman P, Herbert D, Paramasivan CN. Evaluation of the BACTEC radiometric method in the early diagnosis of tuberculosis. Indian Journal of Medical Research. 1998;108:120-7.

11. Metcalfe C, Macdonald IK, Murphy EJ, Brown KA, Raven EL, Moody PCE. The tuberculosis prodrug isoniazid bound to activating peroxidases. Journal of Biological Chemistry. 2008;283:6193-200.

12. Argyrou A, Blanchard JS. Identification of potential new isoniazid targets in Mycobacterium tuberculosis. Abstracts of Papers of the American Chemical Society. 2005;230:U562-U.

13. Argyrou A, Vetting MW, Aladegbami B, Blanchard JS. Mycobacterium tuberculosis dihydrofolate reductase is a target for isoniazid. Nature Structural & Molecular Biology. 2006;13:408-13.

14. Rozwarski DA, Grant GA, Barton DHR, Jacobs WR, Sacchettini JC. Modification of the NADH of the isoniazid target (InhA) from Mycobacterium tuberculosis. Science. 1998;279:98-102.

15. Ngo SC, Zimhony O, Chung WJ, Sayahi H, Jacobs WR, Jr., Welch JT. Inhibition of isolated Mycobacterium tuberculosis fatty acid synthase I by pyrazinamide analogs. Antimicrob Agents Chemother. 2007;51:2430-5.

16. Scorpio A, Zhang Y. Mutations in pncA, a gene encoding pyrazinamidase/nicotinamidase, cause resistance to the antituberculous drug pyrazinamide in tubercle bacillus. Nat Med. 1996;2:662-7.

17. Yendapally R, Lee RE. Design, synthesis, and evaluation of novel ethambutol analogues. Bioorg Med Chem Lett. 2008;18:1607-11.

18. Ziakas PD, Mylonakis E. 4 months of rifampin compared with 9 Months of isoniazid for the management of latent tuberculosis infection: a meta-analysis and cost-effectiveness study that focuses on compliance and liver toxicity. Clinical Infectious Diseases. 2009;49:1883-9.

19. White RJ, Lancini GC, Silvestri.LG. Mechanism of action of rifampin on mycobacterium-smegmatis. Journal of Bacteriology. 1971;108:737-741.

20. Kim H, Kim SH, Ying YH, Kim HJ, Koh YH, Kim CJ, et al. Mechanism of natural rifampin resistance of Streptomyces spp. Systematic and Applied Microbiology. 2005;28:398-404.

21. Noordhuis P, Holwerda U, Van der Wilt CL, Van Groeningen CJ, Smid K, Meijer S, et al. 5-fluorouracil incorporation into RNA and DNA in relation to thymidylate synthase inhibition of human colorectal cancers. Ann Oncol. 2004;15:1025-32.

22. Van Triest B, Pinedo HM, Giaccone G, Peters GJ. Downstream molecular determinants of response to 5-fluorouracil and antifolate thymidylate synthase inhibitors. Ann Oncol. 2000;11:385-91.

23. Dev IK, Yates BB, Leong J, Dallas WS. Functional role of cysteine-146 in Escherichia coli thymidylate synthase. Proc Natl Acad Sci U S A. 1988;85:1472-6.

24. Finer-Moore JS, Santi DV, Stroud RM. Lessons and conclusions from dissecting the mechanism of a bisubstrate enzyme: thymidylate synthase mutagenesis, function, and structure. Biochemistry. 2003;42:248-56.

25. Tong Y, Liu-Chen X, Ercikan-Abali EA, Zhao SC, Banerjee D, Maley F, et al. Probing the folate-binding site of human thymidylate synthase by site-directed mutagenesis. Generation of mutants that confer resistance to raltitrexed, Thymitaq, and BW1843U89. J Biol Chem. 1998;273:31209-14.

26. Hardy LW, Finer-Moore JS, Montfort WR, Jones MO, Santi DV, Stroud RM. Atomic structure of thymidylate synthase: target for rational drug design. Science. 1987;235:448-55.

27. Matthews DA, Appelt K, Oatley SJ, Xuong NH. Crystal structure of Escherichia coli thymidylate synthase containing bound 5-fluoro-2'-deoxyuridylate and 10-propargyl-5,8-dideazafolate. J Mol Biol. 1990;214:923-36.

28. Chattopadhyay S, Moran RG, Goldman ID. Pemetrexed: biochemical and cellular pharmacology, mechanisms, and clinical applications. Mol Cancer Ther. 2007;6:404-17.

29. Curtin NJ, Hughes AN. Pemetrexed disodium, a novel antifolate with multiple targets. Lancet Oncol. 2001;2:298-306.

30. Hanauske AR, Chen V, Paoletti P, Niyikiza C. Pemetrexed disodium: a novel antifolate clinically active against multiple solid tumors. Oncologist. 2001;6:363-73.

31. Li T, Lara PN, Jr., Mack PC, Perez-Soler R, Gandara DR. Intercalation of erlotinib and pemetrexed in the treatment of non-small cell lung cancer. Curr Drug Targets. 2010;11:85-94.

32. Vogelzang NJ, Rusthoven JJ, Symanowski J, Denham C, Kaukel E, Ruffie P, et al. Phase III study of pemetrexed in combination with cisplatin versus cisplatin alone in patients with malignant pleural mesothelioma. J Clin Oncol. 2003;21:2636-44.

33. Farrugia DC, Ford HE, Cunningham D, Danenberg KD, Danenberg PV, Brabender J, et al. Thymidylate synthase expression in advanced colorectal cancer predicts for response to raltitrexed. Clin Cancer Res. 2003;9:792-801.

34. Fizazi K, Doubre H, Le Chevalier T, Riviere A, Viala J, Daniel C, et al. Combination of raltitrexed and oxaliplatin is an active regimen in malignant mesothelioma: results of a phase II study. J Clin Oncol. 2003;21:349-54.

35. Fizazi K, Ducreux M, Ruffie P, Bonnay M, Daniel C, Soria JC, et al. Phase I, dose-finding, and pharmacokinetic study of raltitrexed combined with oxaliplatin in patients with advanced cancer. J Clin Oncol. 2000;18:2293-300.

36. Schmid KE, Kornek GV, Schull B, Raderer M, Lenauer A, Depisch D, et al. Second-line treatment of advanced gastric cancer with oxaliplatin plus raltitrexed. Onkologie. 2003;26:255-8.

37. Rosati G, Rossi A, Germano D, Reggiardo G, Manzione L. Raltitrexed and mitomycin-C as third-line chemotherapy for colorectal cancer after combination regimens including 5-fluorouracil, irinotecan and oxaliplatin: a phase II study. Anticancer Res. 2003;23:2981-5.

38. Lo MC, Aulabaugh A, Jin G, Cowling R, Bard J, Malamas M, et al. Evaluation of fluorescence-based thermal shift assays for hit identification in drug discovery. Anal Biochem. 2004;332:153-9.

39. Niesen FH, Berglund H, Vedadi M. The use of differential scanning fluorimetry to detect ligand interactions that promote protein stability. Nat Protoc. 2007;2:2212-21.

40. Sorrell FJ, Greenwood GK, Birchall K, Chen B. Development of a differential scanning fluorimetry based high throughput screening assay for the discovery of affinity binders against an anthrax protein. J Pharm Biomed Anal. 2010;52:802-8.

41. Uniewicz KA, Ori A, Xu R, Ahmed Y, Wilkinson MC, Fernig DG, et al. Differential scanning fluorimetry measurement of protein stability changes upon binding to glycosaminoglycans: a screening test for binding specificity. Anal Chem. 2010;82:3796-802.

42. Gangjee A, Jain HD, Phan J, Guo X, Queener SF, Kisliuk RL. 2,4-Diamino-5-methyl-6-substituted arylthio-furo[2,3-d]pyrimidines as novel classical and nonclassical antifolates as potential dual thymidylate synthase and dihydrofolate reductase inhibitors. Bioorganic & Medicinal Chemistry. 2010;18:953-61.

43. Jackman AL, Calvert AH. Folate-based thymidylate synthase inhibitors as anticancer drugs. Ann Oncol. 1995;6:871-81.

44. Nijhout HF, Reed MC, Budu P, Ulrich CM. A mathematical model of the folate cycle: new insights into folate homeostasis. J Biol Chem. 2004;279:55008-16.

45. Huang RF, Ho YH, Lin HL, Wei JS, Liu TZ. Folate deficiency induces a cell cycle-specific apoptosis in HepG2 cells. J Nutr. 1999;129:25-31.

46. Theti DS, Jackman AL. The role of alpha-folate receptor-mediated transport in the antitumor activity of antifolate drugs. Clin Cancer Res. 2004;10:1080-9.

VITA

Name:	Wayne Daniel Harshbarger
Address:	Sacchettini Lab Texas A&M University 301 Old Main Dr. BLDG ILSB, Rm 2138 Biochem, Biophys College Station, TX 77843
Email Address:	wayne.harshba@gmail.com
Education:	Bachelor of Science, Virginia Commonwealth University Richmond, Virginia 2006 Master of Science, Chemistry, Texas A&M University, 2011